Investigation of a sensitive, selective and cost-effective electrochemical meso-porous silicon based gas sensor for NO2 detection at room temperature

Khaoula Azaiez, Hela Mhamdi, Rabia Benabderrahmane Zaghouani, Tomas Fiorido, Jean-Louis Lazzari, Marc Bendahan, Wissem Dimassi

Investigation of a sensitive, selective and cost-effective electrochemical meso-porous silicon based gas sensor for NO_2 detection at room temperature

K. Azaiez[1], H. Mhamdi[2], R. Benabderrahmane Zaghouani[2,*], T. Fiorido[3], J.-L. Lazzari[4], M. Bendahan[3], W. Dimassi[1]

[1]*Laboratoire de Nanomatériaux et Systèmes pour Energies Renouvelables, Centre de Recherches et des Technologies de l'Energie, Technopôle de Borj-Cédria, BP, 95 Hammam-Lif, Tunis, Tunisie*

[2]*Laboratoire de Photovoltaïque, Centre de Recherches et des Technologies de l'Energie, Technopôle de Borj-Cédria, BP, 95 Hammam-Lif, Tunis, Tunisie*

[3] *Aix Marseille Univ, CNRS, IM2NP, AMUTech, Marseille, France*

[4]*Aix Marseille Univ, CNRS, CINaM, AMUTech, Marseille, France*

[*]Corresponding author: R. Benabderrahmane Zaghouani

E-mail address: rabia.benabderrahmane@gmail.com

Abstract

This work presents a nitrogen dioxide (NO_2) gas sensor based on porous silicon with improved sensitivity, selectivity, and cost-efficiency. Porous silicon is being researched as an alternative material for gas sensors operating at room temperature (RT), making it suited for low-consumption applications. Meso-porous silicon (meso-PS) films were prepared on p+ type Si (100) using an electrochemical method for NO_2 gas sensing.[ak1]

Morphology, structural and optical properties of meso-PS films were investigated using scanning electron microscope (SEM), X-ray diffractometer (XRD), and UV-Vis spectroscopy. The gas sensing response of meso-PS samples was performed at RT with top parallel Al electrodes in the range of 4 to 10 ppm of NO_2 gas. The tested sensor showed high normalized response (R_{air}/R_{gas} =40 for 4 ppm to 100 for 10 ppm) thanks to its high surface/volume ratio, good repeatability and reversibility, fast response (40 s) and recovery times (18 s), and good selectivity for NO_2 vs. NH_3, O_3 and CO. All these performances obtained at RT are encouraging for low-power devices.

Key words: mesoporous silicon (meso-PS); electrochemical anodization, nitrogen dioxide (NO_2) gas sensor, room temperature (RT); low power

1. Introduction

A variety of sensors are required to meet today's high standards [1-2]. Gas sensors that operate at room temperature and have dynamic features, good sensitivity, and high selectivity are in high demand for environmental and human health protection. In particular, important efforts have been dedicated to silicon nanostructures research for their high potential as a candidate for different applications such as porous silicon [3-4] and silicon nanowires [5-6].

With the rapid rise of industry over the last few decades, the environment has been suffering from severe problems produced by air pollution. These problems cause damaging effects to human health. Nitrogen dioxide (NO_2) is one of the most common atmospheric pollutants. Excessive NO_2 in an atmospheric environment may

cause acid rain, photochemical smog and haze. For this purpose, there has been an increasing demand for high performance gas detection systems.

Since the 1970s, some companies had industrialized sensors, with a trade-off between the different characteristics of the sensor (price, consumption, difficulty of use, sensitivity, stability, size etc.). These sensors were based on metal oxides as sensitive materials. Presenting some attractive properties, including easy operation, convenient fabrication, low cost and good portability, metal oxides have been extensively studied and widely used in the fabrication of gas sensors (MOx sensors) [7-10]. However, MOx sensors always need additional heating to maintain adequate sensitivity, good selectivity and acceptable detection speed, limiting their application. Therefore, the main objectives of the new generation of gas sensors are high sensitivity, selectivity and low consumption. The development of a sensor operating at room temperature (RT) will be an important step forward in the field of gas sensors. The high sensitivity could be reached by increasing the surface/volume ratio.

Porous silicon (PS) is a suitable material for the development of gas sensors for various applications, including environmental monitoring, indoor air quality control, and industrial process control, due to its large specific surface [11-12], low cost, and the simplicity of its set-up [13-16]. [ak2]

Interesting results have been obtained for PS gas sensors detecting NO_2 [16-19], NH_3 [20-21] and CO_2 gases [22-23]. M. Sik Choi et al. [17] have studied PS fabricated by electrochemical etching during different times (30, 60, and 90 min) for NO_2 detection. The PS sensor etched during 60 min presented the highest response of 9.56 towards 10 ppm of NO_2 gas with fast response-recovery times. The NO_2 PS sensor was studied for other interfering gases (acetone, ethanol, CO, SO_2) showing a high selectivity to NO_2 gas. Also, M. Li et al. [18] have investigated the sensing performances of mesoporous silicon to 2 ppm of NO_2 gas using electrochemical etching process presenting a response value of 2,5.

In this work, meso-PS gas sensing was studied towards NO_2, O_3, NH_3 and CO gases at room temperature and has exhibited excellent selectivity for NO_2 gas with a high sensing response not reported yet in the literature and good response repeatability.

2. Experimental details:

a. Sample preparation:

Meso-porous silicon (meso-PS) sample was prepared by electrochemical anodization process (Figure.1) of p^+ type mono-crystalline Si wafer (100) with a resistivity of 0.01–0.02 Ohm.cm. An electrolyte composed of HF (40%)/C_2H_5OH (99.9%) ≡ (1:1) mixture solution under 30mA/cm^2 etching current density for 5 min was used to anodize the silicon substrate. The main parameters for the porous layer are controlled by the porosity and the layer thickness. Porosity is defined as the measure of the percentage of voids in a porous structure. The gravimetric approach is an easy way to determine the average porosity (P) of the prepared PS.

$$\mathbf{P} = \frac{m_1 - m_2}{m_1 - m_3}$$

Where m_1 and m_2 represent the mass of the mesoporous silicon sample before and after the anodization process, respectively. "m_3" is the mass obtained after removing the porous layer with NaOH solution. It is about 68%. The thickness of the porous silicon (PS) layer was measured with ImageJ software using the SEM cross-sectional view shown in Figure 3b. Its value is 5 µm. These parameters are critical aspects that can influence gas sensing performance. [ak3]

Al electrodes were deposited on the top surface of meso-PS gas sensor using thermal evaporation method with a thickness of about 100 nm in a parallel configuration.

b. Characterization methods

The meso-PS morphology was performed by the scanning electron microscopy (SEM JEOL JSM-6340F). The crystal structure of as-prepared films was examined by X-ray diffractometer (X'PERT MRD (PanAlytical)). For surface reflectivity measurements, a PerkinElmer Lambda 950 UV/VIS/NIR spectrometer equipped with an integrating sphere was used.

c. Gas-sensing measurements

The gas sensing performances of the sensors were evaluated in a dynamic gas-sensing test system. The sensor was placed on a heating plate connected to a temperature controller used to adjust the operating temperature. The sensor dynamic response was obtained by measuring the sensor resistance change under gas. The gas-sensing test system is composed of different parts: gas cabinet, dry air generator, mass flow control, and ozone generator, test chamber with a temperature regulator, control and data acquisition system (Figure.2 (a)).
Figure.2 (b) shows the photography of the test used. In this work, the gas sensor response is defined by the following equation:

$$S = \frac{R_a}{R_g} \qquad \text{(Eq. 1)}$$

Where R_a and R_g are, respectively, the sensor resistance measured in air and under gas. The sensor performance is also described by the response and recovery times. The response time is defined as the time required for the sensor to reach 90% of the total response after gas exposure. Accordingly, recovery time is the time necessary to return to 90% of the original baseline signal after gas removal. In this work, the sensing properties of meso-PS sample towards nitrogen dioxide (NO_2) and interfering gases as ozone (O_3), ammonia (NH_3), and carbon monoxide (CO) gases were evaluated. The meso-PS sensor is tested toward exposed gas at room temperature (25 ± 2°C) under variable gas concentrations.

3. Results and discussion:

a. Sample characterization:

The porous silicon layer was analyzed with Scanning Electron Microscopy to explore the morphology of the meso-PS, as displayed in Figure.3. The SEM top view of meso-PS (Figure.3 (a)) shows homogeneous pores with average diameters ranging between 7 and 15 nm confirming that the synthesized silicon layer is mesoporous. A cross-section SEM image of the sample (Figure.3 (b)) also enables for the measurement of the porous layer's thickness, which is around 5 µm.

Figure.4 shows the X-ray diffraction spectrum of meso-PS. We note the existence of two Bragg peaks: The most intense peak corresponds to the silicon substrate, and the second peak, located at a smaller Bragg angle, is relative to the PS layer. The reduction in the size of the silicon crystals towards the nanometric scale causes a slight expanding of the diffraction peaks. In addition, the FWHM of the PS peak is not significantly different from that of crystalline silicon, which confirms that the PS skeleton has the characteristics of an almost perfect crystal.

Figure.5 shows the reflectivity spectra of silicon before and after porosification, performed in the range of 300 nm to 1200 nm. The reflectivity drops dramatically from 56% for the silicon sample to around 38% for the PS sample. This reduction is due to the rough and irregular shape of the nano-structured surface of meso-PS compared to that of bulk silicon.

b. Gas sensing properties:

Table.1 illustrates the different gas sensing characteristics. Mesoporous silicon sensor showed a high sensitivity of $R_a/R_g = 40$ for 4ppm of NO_2 justified by the high porosity of 68%. In fact, the high surface roughness, the high porosity, and the optimized morphology of meso-PS, make the adsorption rate between the porous layer and the NO_2 gas molecules more effective. In order to show the stability of the sensor, the gas testing was repeated towards 4 ppm of NO_2 at RT for four cycles (Figure.6). A complete recovery of initial resistance for each test is observed. Meso-PS sensor presented excellent stability of response. Further measurements were taken for different NO_2 concentrations (4, 6, 8 and 10 ppm) during an exposure time of 1 min at RT (Figure.7), where for 4, 6, 8 and 10 ppm NO_2 gas, the response values are 40, 70, 90 and 100 respectively. As the NO_2 concentration increased from 4 ppm to 10 ppm, as shown in Figure.7, the meso-PS sensor response also increased from 40 to 100 respectively, indicating that the sensor may be able to detect NO_2 gas at RT at low concentrations. This result is very significant as compared to the results shown in the literature. [18-19]

Fig. 7 depicts the variation in the meso-PS sensor response exposed to a different NO2 concentration during an exposure time of 1 minute at room temperature. It indicates that the meso-PS sensor can detect trace amounts of NO_2 as low as 4 ppm and exhibited a good response in the range of 4–10 ppm at RT.

As the NO_2 concentration increased from 4 ppm to 10 ppm, the meso-PS sensor response also increased from 40 to 100 respectively, indicating that the sensor may be able to detect NO_2 gas at RT at low concentrations. This result is very significant as compared to the results shown in the literature **(table.2).** As an example, S. Peng et al. [19], studied the gas sensing properties of macro- and meso-porous silicon (PS) at room temperature, examining the influence of microstructure on sensitivity. They reported a response of 188 to 50 ppm of NO_2 gas. However, considering the health effects of NO_2, there are worldwide standards for the concentration of NO_2 in the air that must not be exceeded. As a result, the detection measure at high concentrations is not of great interest.

Moreover, the response of porous silicon is dependant on many parameters such as the electrode configuration [26], the porosity, the porous layer thickness [27], the fabrication technique [15] justifying the difference in the obtained results.

This remarkable response can be documented by the optimized morphology of meso-PS sensor; its high porosity and large surface area. As a result, such nanostructures may facilitate the rapid transfer of mobile charge carriers and active sites during gas adsorption and desorption. Moreover, in comparison to compact thin layers, porous film microstructures have substantially better gas sensitivity thanks to the presence of grain boundaries in all directions, providing additional surface area for reactions with gas molecules to occur. The presence of gas molecules, on the other hand, affects just a small portion of the exposed surface area in a compact film. As a result, porous films are better for gas sensing. [ak4]

The selectivity of a gas sensor is a very important property. In this work, the gas selectivity of meso-PS sensor was studied for 4 ppm of different interfering gases (NH_3, CO and ozone O_3) (Figure.8). PS sensor showed the highest response for NO_2 gas, a very low response for O_3 and no response for NH_3 and CO. The synthesized meso-PS sensor presented an excellent selectivity for NO_2 gas. It could be due to porous silicon's high penetration coefficient for NO_2 gas.

Gas sensor response is due to the adsorption-desorption reaction between materials surface and gas molecules. It is found that the surface states and oxygen adsorption play an important role in NO_2 detection. NO_2, acts as an oxidizing gas, will capture the electrons from the meso-PS sensor. Figure.9 presents the NO_2-sensing

mechanism at RT of the presented sensor. In the first step, the atmospheric oxygen molecules, adsorbed onto the meso-PS surface in the form of O_2^- , are extracting electrons from the meso-PS ((Eq. (2)–(3)). In the case of the p-type porous silicon sensor, it leads to the formation of a hole accumulation layer (Figure 9 (b)), which reduces the material's resistance [24].

$$O_2(gas) \rightarrow O_2(ads) \quad \text{(Eq. 2)}$$

$$O_2(gas) + e^- \rightarrow O_2^-(ads) \quad \text{(Eq. 3)}$$

It is well known that NO_2 is a strong oxidizing gas acting as acceptor centers. In the second step, when the meso-PS sensor is exposed to NO_2, the gas molecules may be directly adsorbed onto the PS surface by trapping electrons (Eq. 4), and interact with the chemisorbed oxygen O_2^- ((Eq. 5) [24]. The resistance of meso-PS will decrease. This is explained by the increase in hole concentration in the shell layer due to the ionosorption of oxidizing gas (Figure.9 (c)).

$$NO_2(gas) + e^- \rightarrow NO_2^-(ads) \quad \text{(Eq. 4)}$$

$$NO_2(gas) + O_2^-(ads) + 2e^- \rightarrow NO_2^-(ads) + 2O^-(ads) \quad \text{(Eq. 5)}$$

4. Conclusion :

In summary, we have synthesized meso-PS sample using electrochemical anodization technique. We focused, first, on the study of porous silicon morphological, structural and optical properties using scanning electron microscope (SEM), X-ray diffraction (XRD) and UV-Vis spectroscopy. The gas sensing properties of meso-PS sensor were studied at room temperature. This work demonstrates the highly sensitive response of 40 towards 4 ppm of NO_2 with fast response-recovery times. The tested sensor presented good selectivity for NO_2 vs. NH_3, O3 and CO. These results exhibit the real field application of meso-PS as highly sensitive, selective NO_2 gas sensor and instantly regenerated without heating. Therefore, the meso-PS based sensor systems introduce a novel strategy for the design and construction of a promising, low-cost, lower-power and simple gas sensor with excellent performance for low concentrations of NO_2 detection. In further work, the effect of relative humidity and storage on the fabricated sensor would be studied.

References

[1] W. Zhao, R. Yan, H. Li, K. Ding, Y. Chen, D. Xu, Highly sensitive NO2 gas sensor with a low detection limit based on Pt-modified MoS2 flakes, Materials Letters, 330, 133386 (2023)

[2] P. Bharathi, S. Harish, M. Shimomura, M. Krishna Mohan, J. Archana , M. Navaneethan, Controlled growth and fabrication of edge enriched SnS2 nanostructures for room temperature NO2 gas sensor applications, Materials Letters 335, 133691(2023).

[3] R. Benabderrahmane Zaghouani, M. Alaya, H. Nouri, J.-L. Lazzari, W. Dimassi, Study of WO3-decorated porous silicon and Al2O3-ALD encapsulation, Journal of Materials science: Materials in Electronics, 29 (2018), p. 17731.

[4] J. Duan, K.Kang , P. Li, W. Zhang, X. Li, J. Wang , Y. Liu, the design and regulation of porous silicon-carbon composites for enhanced electrochemical lithium storage performance, J. Ind. Eng. Chem. 131, 410-421 (2024).

[5] R. Benabderrahmane Zaghouani, M. Y. Tabassi, K. Khirouni, W. Dimassi, Vapor–liquid–solid silicon nanowires growth catalyzed by indium: study of indium oxide effect, Journal of Materials Science: Materials in Electronics, 30, 9758 (2019).

[6] M. Y. Tabassi, R. Benabderrahmane Zaghouani, M. Khelil, K. Khirouni, W. Dimassi, Study of indium catalyst thickness effect on PECVD-grown silicon nanowires properties, Journal of Materials Science: Materials in Electronics, 13, 9717 (2017).

[7] J. Zhao, M. Hu, Y. Liang, Q. Li, X. Zhang and Z. Wang; A room temperature sub-ppm NO2 gas sensor based on WO3 hollow spheres; New J. Chem. 44, 5064(2020).

[8] A. I. Khudadad, A. A. Yousif, H. R. Abed; Effect of heat treatment on WO3 nanostructures based NO2 gas sensor low-cost device; Materials Chemistry and Physics. 269, 124731 (2021).

[9] H. Mhamdi, R. B. Zaghouani, T. Fiorido, J. L. Lazzari, M. Bendahan, W. Dimassi, Study of n-WO3/p-porous silicon structures for gas-sensing applications, J. Mater. Sci.: Mater. Electron. 31, 7862 (2020).

[10] A. Staerz, S. Somacescu, M. Epifani, T. Kida, U. Weimar and N. Barsan; WO3 Based Gas Sensors: Identifying Inherent Qualities and Understanding the Sensing Mechanism; ACS Sens. 6, 1624 (2020).

[11] K. Azaiez, R.B. Zaghouani, S. Khamlich, H. Meddeb, W. Dimassi, Enhancement of porous silicon photoluminescence property by lithium chloride treatment, Appl. Surf. Sci. 441, 272(2018).

[12] R. B. Zaghouani, M. Alaya, H. Nouri, J. L. Lazzari, W. Dimassi, Study of WO3-decorated porous silicon and Al2O3-ALD encapsulation, J. Mater. Sci.: Mater. Electron. 27, 17731(2018).

[13] Alwan, A.M., Abed, H.R., Rashid, R.B., Enhancing the Temporal Response of Modified Porous Silicon-Based CO Gas Sensor, Solid-State Electronics 181, 108019(2021).

[14] L. Boarino, M. Rocchia, C. Baratto, A. M. Rossi, E. Garrone, S. Borini, F. Geobaldo, E. Comini, G. Faglia, G. Sberveglieri and G. Amato; Towards a deeper comprehension of the interaction mechanism between mesoporous silicon and NO2, Physic. Stat. sol. 182, 465(2000).

[15] H. Mhamdi, K. Azaiez, T. Fiorido, R. B. Zaghouani, J.L. Lazzari, M. Bendahan, W. Dimassi, Room temperature NO2 gas sensor based on stain-etched porous silicon: Towards a low-cost gas sensor integrated on silicon, Inorganic Chemistry Communications. 139, 109325 (2022).

[16] W. Bdaiwi, Fabrication of Gas Sensor Device for H2 and NO2 from Porous Silicon, Appl. Phys. Res. 5, 7 (2015).

[17] M. Sik Choi, H. Gil Na, A. Mirzaei, J. Hoon Bang, W. Oum, S. Han, S. Choi, M. Kim, C. Jin, S. Kim, H. Woo Kim, Room-temperature NO2 sensor based on electrochemically etched porous silicon, J. Alloys Compd. 811, 151975(2019).

[18] M. Li, M. Hu, W. Yan, S. Ma, P. Zeng, Y. Qin, NO_2 sensing performance of p-type intermediate size porous silicon by a galvanostatic electrochemical etching method; Electrochimica Acta. 113, 354 (2013).

[19] S. Peng, H. Ming, L. Ming-Da, M. Shuang-Yun, Microstructure, Electrical and Gas Sensing Properties of Meso-Porous Silicon and Macro-Porous Silicon, Acta Phys. Chim. Sin. 28 (2), 489-493 (2012)

[20] B.A. Khaniyev , Y. Sagidolda , K.K. Dikhanbayev , A.O. Tileu & M.K. Ibraimov, High sensitive NH3 sensor based on electrochemically etched porous silicon; Cogent Engineering. 7, 1810880 (2020).

[21] A. A. Yousif, H. R. Abed, A. M. Alwan; Different Electrode Configurations for NH3 Gas Sensing Based on Macro Porous Silicon Layer; Springer Nature B.V. 14, 3269(2021).

[22] R. A abbas, A. M Alwan, Z. T Abdulhamied, Synthesis and characterization of porous silicon gas sensors, Journal of Physics: Conf. Series. 1003, 012087 (2018).

[23] A Ghaderi, J Sabbaghzadeh, L Dejam et al, Nanoscale morphology, optical dynamics and gas sensor of porous silicon. Scientific Reports, vol. 14, no 1, p. 3677 (2024).

[24] N.K. Ali, M.R. Hashim, A.A. Aziz, Effects of surface passivation in porous silicon as H2 gas sensor, Solid-State Electron. 52, 1071 (2008).

[25] C.M. Ghimbeu, J. Schoonman, M. Lumbreras, M. Siadat, Electrostatic spray deposited zinc oxide films for gas sensor applications, Appl. Surf. Sci. 253, 7483 (2007).

[26] A.A. Yousif, H. R. Abed, A. M. Alwan, Different electrode configurations for NH3 gas sensing based on macro porous silicon layer, Silicon, 14, 3269(2022).

[27] B. A Khaniyev, Y. Sagidolda, K. K. Dikhanbayev, A. O. Tileu, M. K. Ibraimov, High sensitive NH3 sensor based on electrochemically etched porous silicon, Cogent Engineering, 7, 1810880 (2020).

[28] W. Yan, M. Hu, P. Zeng, S. Ma, M. Li, Room temperature NO2-sensing properties of WO3 nanoparticles/porous silicon, Applied Surface Science, 292, 551(2014).

Acknowledgements:

The authors would like to thank *Damien Chaudanson* and *Alexandre Altié* for SEM measurements done at the Centre Interdisciplinaire de Nanoscience de Marseille (CINaM).

Statements & Declarations

Funding:

This work was supported by the bilateral Tuniso-French PHC-UTIQUE project (Code CMCU: 20G1108-Code Campus France: 44146SM).

Conflict of interest statement:

The authors declare that they have no relevant financial or non-financial interests to disclose.

Author Contributions

All authors contributed to the study conception and design. Material preparation, data collection and analysis were performed by Khaoula AZAIEZ, Rabia Ben Abderrahmane and Hela Mhamdi. The first draft of the manuscript was written by Khaoula AZAIEZ and Hela Mhamdi and all authors commented on previous versions of the manuscript. All authors read and approved the final manuscript."

Data availability

The data that support the findings of this study are available from the corresponding author upon reasonable request.

Figure Caption

Fig.1 Electrochemical Anodization cell.

Fig.2 (a) Schematic illustration and (b) photography of the gas-sensing test system.

Fig.3 SEM top views (a) and cross sectional views (b) of meso-PS sample.

Fig.4 X-Ray diffractogram of meso-PS sample.

Fig.5 Reflectivity spectra of silicon and porous silicon samples.

Fig.6 Response of the meso-PS sensor exposed to 4 ppm of NO_2 at RT: (a) variation for successive cycles (b) enlargement of one cycle

Fig.7 Response of meso-PS sensor as function of NO_2 gas concentration.

Fig.8 Response of meso-PS sensor for different gas.

Fig.9 Sensing mechanism of meso-PS sensor.

Table:

Table 1 The different properties of meso-PS layer.

Table 2 Comparison with previous works based on porous silicon gas sensors.

Table 1: The different properties of meso-PS layer

Sensor	Porosity (%)	Porous thickness layer (µm)	Response $R = R_a/R_g$	Response time (s)	Recovery time (s)
Meso-PS	68 %	5 µm	40	40	18

Table 2: Comparison with previous works based on porous silicon gas sensors.

Sensor	Gas	Gas concentration (ppm)	Temperature (°C)	Response $R = R_a/R_g$	Fabrication method	Ref
Meso-PS	NO2	4	RT	40	Electrochemical anodization	This work
Macro-PS	NO2	4	RT	2,35	Stain etching	[15]
Nano-PS	NO2	4	RT	1,5		
Meso-PS	NO2	2	RT	2,5	Electrochemical anodization	[18]
Macro-PS	NO2	3	RT	7,55		[17]
Macro-PS	NH3	150	RT	3.5	laser-assisted etching	[26]
Nano-PS	NH3	0.1	RT	33.25	Electrochemical anodization	[27]
WO3/nano-PS	NO2	4	100 °C	1.4	Stain etching	[9]
	NH3	100	100 °C	2.23		
WO_3 /(Macro-PS	NO2	2	RT	3,37	electrochemical corrosion	[28]

Fig.1 Electrochemical Anodization cell

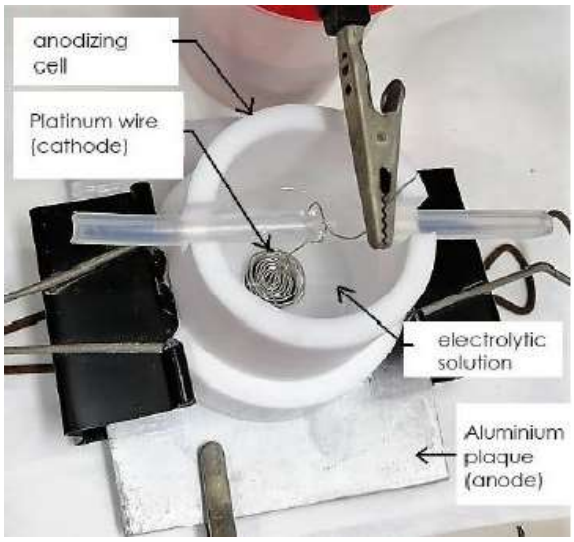

Fig.2 (a) Schematic illustration and (b) photography of the gas-sensing test system

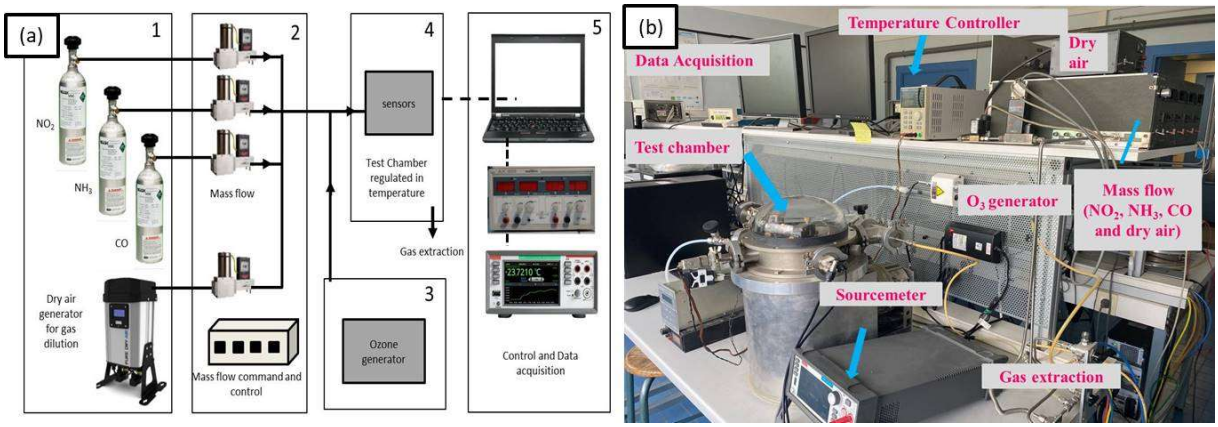

Fig.3 SEM top views (a) and cross sectional views (b) of meso-PS sample

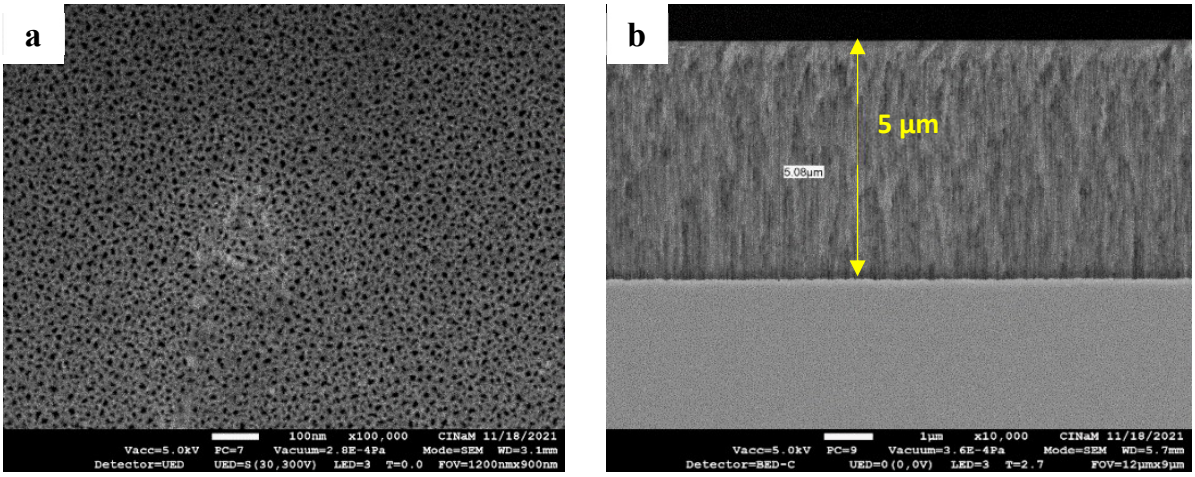

Fig.4 X-Ray diffractogram of meso-PS sample

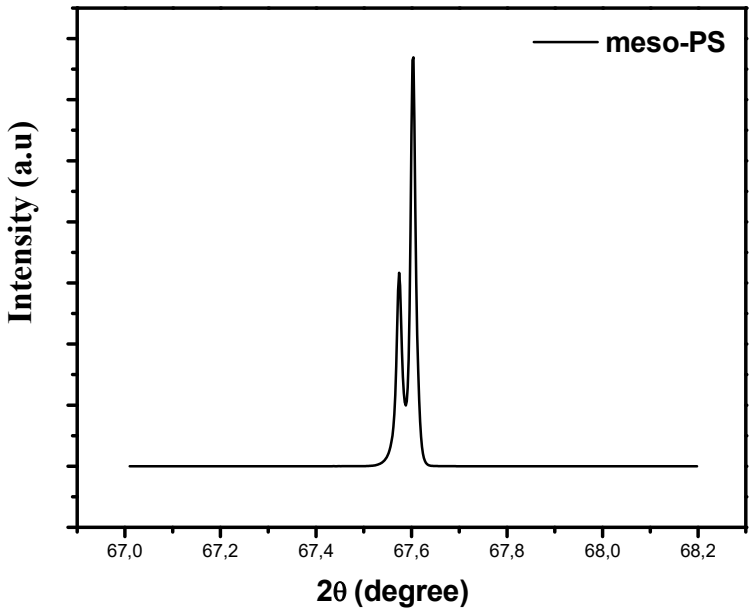

Fig.5 Reflectivity spectra of silicon and porous silicon samples

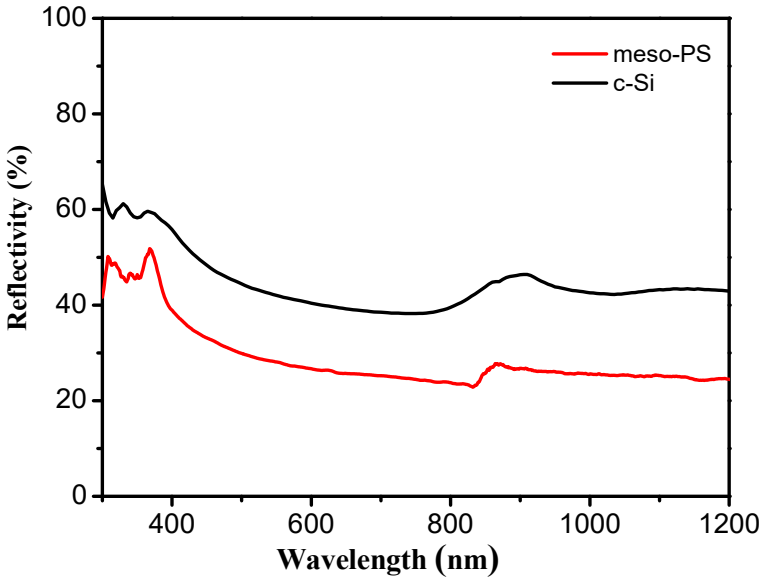

Fig.6 Response of the meso-PS sensor exposed to 4 ppm of NO_2 at RT (a) variation for successive cycles (b) enlargement of one cycle

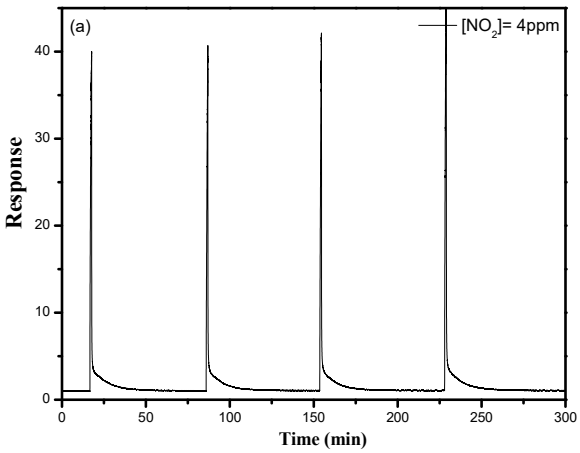

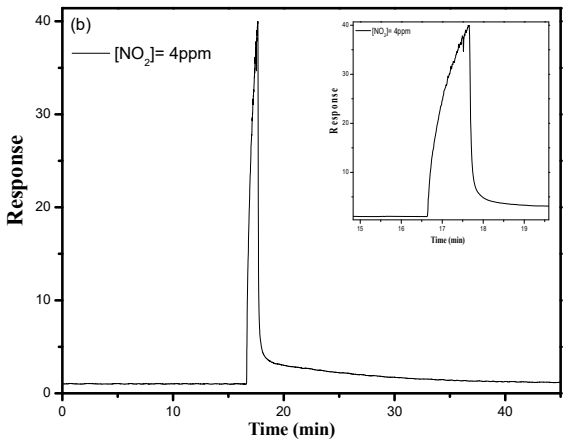

Fig.7 Response of meso-PS sensor as function of NO_2 gas concentration

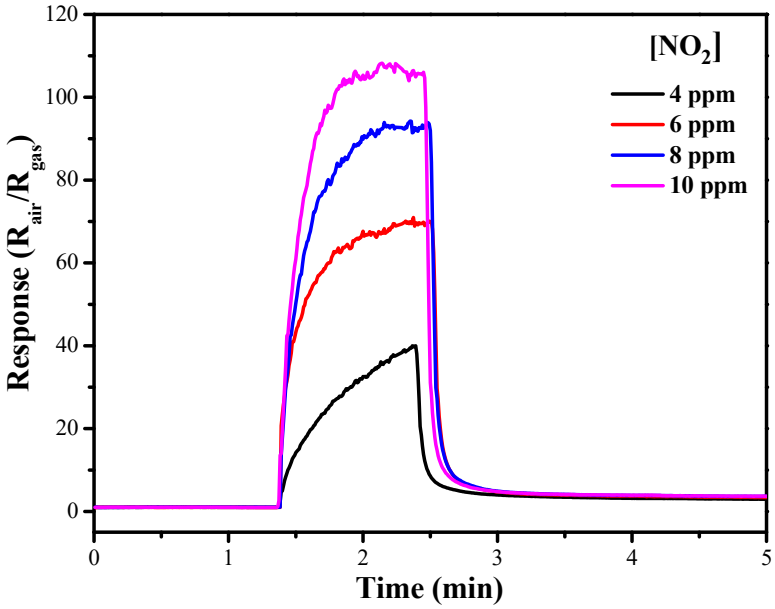

Fig.8 Response of meso-PS sensor for different gas

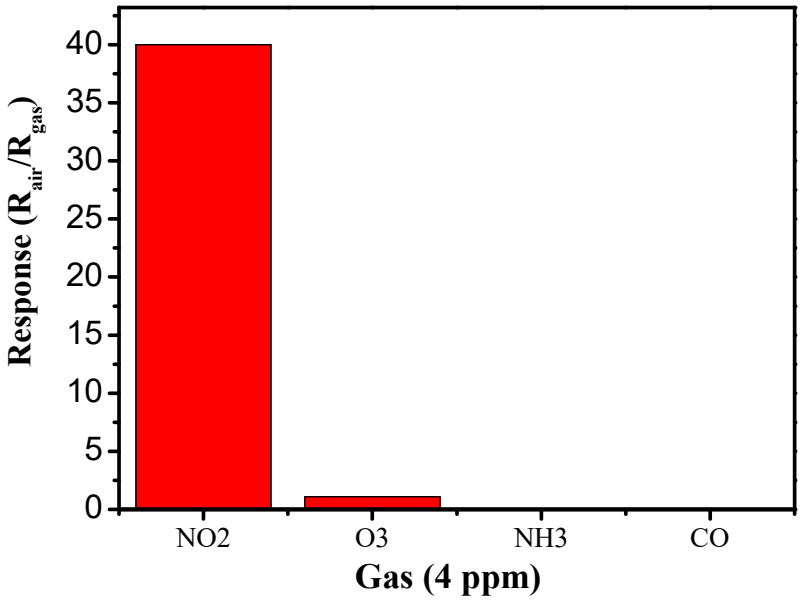

Fig.9 Sensing mechanism of meso-PS sensor